Spin Stripe Fluctuations in Antiferromagnetic $Pr_{2-x}Sr_xNiO_{4+\delta}$

Avishek Maity,[1,*] Rajesh Dutta,[2,3,†] and Werner Paulus[4]

[1]*Heinz Maier-Leibnitz Zentrum (MLZ), Technische Universität München, 85747 Garching, Germany*
[2]*Institut für Kristallographie, RWTH Aachen Universität, 52066 Aachen, Germany*
[3]*Jülich Centre for Neutron Science (JCNS) at Heinz Maier-Leibnitz Zentrum (MLZ), 85747 Garching, Germany*
[4]*ICGM, Université de Montpellier, CNRS, ENSCM, 34293 Montpellier, France*

We report inelastic neutron scattering study of the antiferromagnetic spin stripe fluctuations above the spin stripe melting temperature $T_{so} \approx 190$ K in the hole doped $Pr_{2-x}Sr_xNiO_{4+\delta}$ with stripe incommensurability $\epsilon = 0.33$. The fluctuations are non-dispersive and detected upto 10 meV at the incommensurate wave vector indicating a persisting instantaneous spin and charge stripe correlation above T_{so}, while they are strongly diminished already below the charge stripe melting temperature $T_{co} \approx 255$ K which indicates that static charge stripe order is essential for the dynamical spin stripe correlation to exist. Furthermore it also suggests that the presence of spin stripe fluctuations is not a prerequisite for the formation of static charge stripes.

I. INTRODUCTION

Spin and charge stripe correlation and their dynamics have been well explored in the superconducting La-based 214-cuprates and other hole doped 214-nickelates to understand the possible role of stripe correlation in the high-T_c superconductivity [1–10]. Beyond a critical hole doping concentration the charge carriers segregate in the form of stripes and act as antiphase domain walls inbetween the antiferromagnetic spin stripes [1, 5]. The incommensurabilities of the stripes as well as their ordering temperatures directly depend on the hole doping concentrations $n_h = x + 2\delta$ [11, 12]. Stripes in nickelates are localized over a wide range of hole doping concentrations [12]. In contrast, stripes in cuprates exist almost in a liquid like fluctuating state and play an important role in the spin fluctuation mediated high-T_c superconductivity [13–17]. It has been also suggested that the presence of low energy spin stripe fluctuations acts as a driving force behind the charge nematic ordering in electronic liquid crystal state of high-T_c cuprates [15, 17, 18].

Considering the amount of experimental work put forward characterizing the spin stripe ordering and dynamics of 214-nickelates [6–10] and theoretical calculations presenting various aspects of the ground state [19–21], what remains less explored is the fluctuating state of the spin stripes including their dynamical correlation from which the long range static spin stripes develop on cooling. Recent studies show the existence of a strong charge stripe fluctuations above the spin stripe melting temperature T_{so}. The presence of such fluctuating charge stripes in $La_{2-x}Sr_xNiO_4$ with $x = 0.33$ have been inferred from the temperature dependence of the atomic displacement parameters [22]. While a direct evidence of dynamic charge stripes has been reported by Anissimova et al. for $La_{2-x}Sr_xNiO_4$ with $x = 0.33$ and 0.25 using inelastic neutron scattering (INS) study [23]. Zong et al. reported the presence of the charge stripe fluctuation dispersion in a $La_{2-x}Sr_xNiO_4$ sample with $x = 0.25$ where the anisotropy in the measured dispersion reveals the compelling evidence of the presence of electronic nematic order [24]. In the same way the investigation on the spin stripe excitations just above the spin stripe melting temperature may also give interesting information on spin stripe fluctuations and their possible interaction with the charge stripes.

In this paper, we present an INS study of the spin stripe fluctuations at temperatures above T_{so} in $Pr_{2-x}Sr_xNiO_{4+\delta}$ ($x \approx 0.125, \delta \approx 0.1$) with $\epsilon = 0.33$. In the present case, we investigate the regime where the static charge stripes are fully established without the presence of a static spin stripe correlation. We show that the dynamical correlation of the non-dispersive spin stripe fluctuations persists upto a maximum energy 10 meV at the incommensurate wave vector and strongly diminished already below the charge stripe melting temperature T_{co} which clearly indicates that the formation of static charge stripe order is not driven by the spin stripe fluctuations, rather the presence of static charge stripe order is essential for dynamical spin stripe correlations to exist.

II. EXPERIMENTAL DETAILS

INS measurements were performed using the thermal neutron triple axis spectrometer PUMA at Heinz Maier-Leibnitz Zentrum, Germany [25]. The high quality single crystal of $Pr_{2-x}Sr_xNiO_{4+\delta}$ used for the experiment was grown by travelling solvent floating zone method using a mirror furnace. INS data were collected on a $10 \times 6 \times 3$ mm^3 single crystal with a fixed final energy $E_f = 14.68$ meV of neutrons. We have used the pyrolytic graphite (PG 002) crystals monochromator and analyzer to select the incident and final energies of neutrons. A PG filter was used in between the sample and analyzer to suppress the higher order harmonics from the scattered neutron beam. The crystal was aligned to measure the INS in the $(hk0)$ scattering plane. Optimally focused

* avishek.maity@frm2.tum.de
† rajesh.dutta@frm2.tum.de

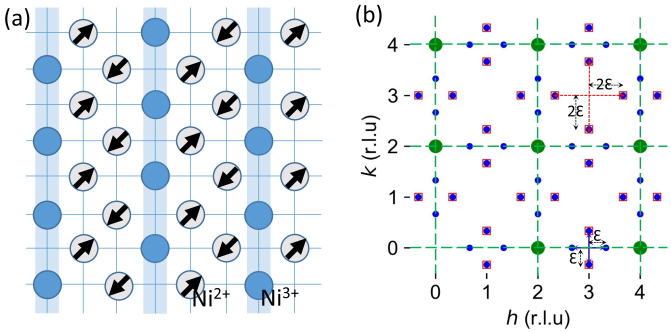

FIG. 1. (a) Schematic representation of the spin and charge stripes in real space with stripe incommensurability $\epsilon = 0.33$. The stripes are running parallel to the *b*-axis and diagonal to the Ni-O bond. For the twin domain the spin and charge stripes are just rotated by 90°. (b) Simulation of the spin (in blue dots) and charge (in red squares) stripe reflection positions including the main Bragg reflections (in green dots).

monochromator and analyzer configuration of the spectrometer with open collimation was used for both elastic and inelastic measurements.

III. RESULTS AND DISCUSSION

We interpret our results in the pseudotetragonal F4/*mmm* unit cell with lattice parameters $a = b \approx 5.41$ and $c \approx 12.45$ Å. The stripes form along the diagonal direction with respect to the Ni–O bonds *i.e.* parallel to the h or k reciprocal directions. Then the spin and charge stripe wave vectors are indicated in terms of incommensurability ϵ as $q_{so} = (\epsilon, 0, 0)$ and $q_{co} = (2\epsilon, 0, 1)$ respectively where the coordinates are in reciprocal lattice units $(2\pi/a, 2\pi/b, 2\pi/c)$.

We have determined the stripe incommensurability ϵ through the scan along h and k directions from the antiferromagnetic zone center. For our measurements on the single crystal of $Pr_{2-x}Sr_xNiO_{4+\delta}$ we have obtained the stripe incommensurability $\epsilon = 0.33$. The schematic for spin and charge stripes are presented in Fig. 1(a) with incommensurability $\epsilon = 0.33$ for a single domain. With $\epsilon = 0.33$ the spin and charge stripe wave vectors coincide as presented in the Fig. 1(b). All the satellite reflections corresponding to the charge stripes overlap with spin stripes, excluding the spin stripe satellites which are located on the dashed green lines connecting the main Bragg reflections. The samples with $\epsilon = 0.33$ show relatively high spin stripe (T_{so}) and charge stripe (T_{co}) ordering temperatures with respect to the samples with higher or lower incommensurabilities [11, 12]. We have performed a set of elastic scans through the satellites corresponding to the spin and charge stripes to determine T_{so} and T_{co}. Fig. 2(a) shows the scans through a spin stripe satellite position $(0.67, 0, 0)$, whereas Fig. 2(b) presents the scans through the spin and charge stripe overlapped satellite position $(3, -0.33, 0)$. Since the spin

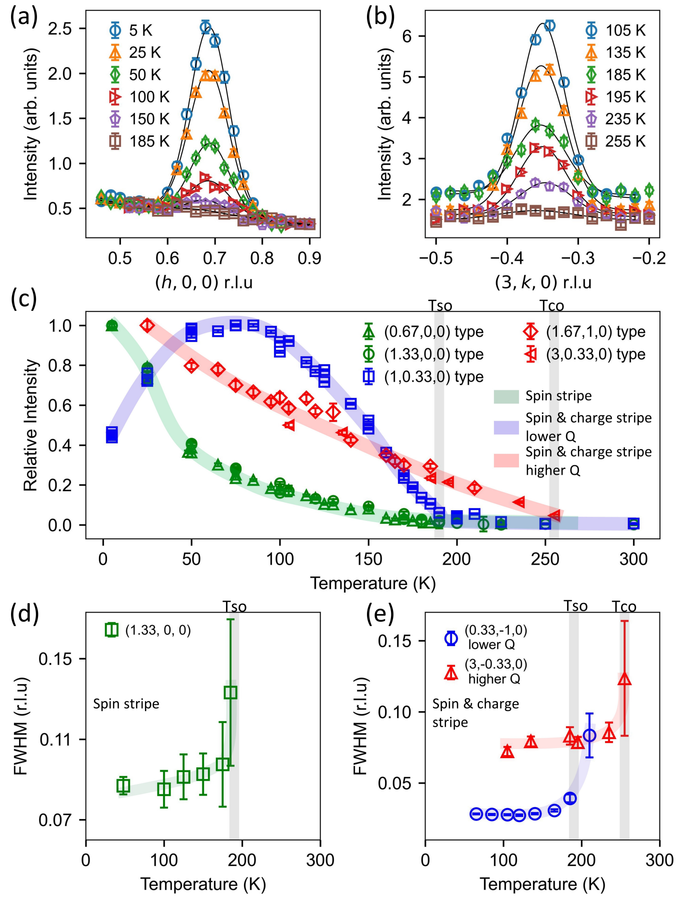

FIG. 2. (a) T-dependent scans through the spin stripe satellite $(0.67, 0, 0)$. (b) T-dependent scans through the spin and charge stripe overlapped satellite $(3, -0.33, 0)$. (c) T-dependence of the relative intensities from the spin and charge stripe reflections from different Brillouin zones. (d) T-dependent full width at half maxima (FWHM) of the spin stripe satellite $(1.33, 0, 0)$. (e) T-dependent FWHM of the spin and charge stripe overlapped satellites $(0.33, -1, 0)$ at lower Q and $(3, -0.33, 0)$ at higher Q. The fainted lines are for the guide to eye.

and charge stripe satellites are overlapped at certain positions for $\epsilon = 0.33$, it needs extra care to separate the scattering intensities related to the spin and charge stripe ordering to determine the respective ordering temperatures.

The scattering intensities from spin stripes are higher at low Q and decrease at high Q following the magnetic form factor. Whereas the scattering intensities from charge stripes can not be measured directly by neutrons but can be detected through the associated lattice deformations for which the intensities grow at high Q [23, 24]. We performed scans through the spin and charge stripe satellites in several Brillouin zones (see Fig. S1 in supplementary information [26]) to determine the relative intensity fall of the static spin and charge stripe satellites as a function of temperature (T) as presented in the Fig 2(c). The integrated intensities of the spin stripe satellite positions at $(0.67, 0, 0)$ with $Q = 0.77$ Å^{-1} and $(1.33, 0, 0)$ with $Q = 1.55$ Å^{-1} drop close to zero approximately at 190 K. This indicates the spin stripe melting temperature $T_{so} \approx 190$ K. The weak non-vanishing intensities above T_{so} may possibly come from the integrated intensity of the low energy spin fluctuations close to elastic line [27]. Similarly the integrated intensity measured at the spin and charge stripe overlapped satellite position at $(1, 0.33, 0)$ with relatively lower Q value $Q = 1.23$ Å^{-1} as well drops close to zero at around 190 K. This implies that at this Q the magnetic scattering intensities from the spin stripes still dominate over the intensities from charge stripes. Nonetheless one can notice that the magnetic intensities for the $(1, 0.33, 0)$-type satellites peak at ~ 60 K showing a different T-dependence compared to the magnetic intensities measured at $(0.67, 0, 0)$-type satellites. This can be related to the change in spin orientation in the stripes [28]. The T_{so} can be aswell identified from the estimated peak width at $(1.33, 0, 0)$ and $(0.33, -1, 0)$ as a function of temperature in Fig. 2(d,e) which clearly shows an increase in FWHM as the magnetic intensities start to drop [27]. For the measurements at relatively higher Q values at the spin and charge stripe overlapped satellite positions $(1.67, 1, 0)$ with $Q = 2.26$ Å^{-1} and $(3, 0.33, 0)$ with $Q = 3.52$ Å^{-1}, the scattering intensities related to static charge stripes start to dominate as the intensities persist upto 255 K as presented in Fig. 2(c) which can be considered as the charge stripe melting temperature T_{co} where the corresponding peak width at $(3, -0.33, 0)$ also shows a clear increase as shown in Fig. 2(e).

We have further investigated the T-dependence of the low energy (E) inelastic signal at and above the spin stripe ordering temperature $T_{so} \approx 190$ K to have an estimation of the dynamical contribution related to the short range spin stripe fluctuations and dynamical correlation coming from existent charge stripe ordering. Fig. 3(a) shows the Bose corrected inelastic scans at $E = 3$ meV at the spin and charge stripe overlapped satellite position $(3, -0.33, 0)$ as a function of temperature. Clearly the Q-integrated $\chi''(\omega)$ decreases monotonously above T_{so} and vanishes close to the T_{co} as presented in Fig. 3(b). The monotonous decrease of the inelastic signal without presenting any upturn while increasing the temperature suggests the inelastic signal is predominantly contributed by the spin stripe fluctuations rather than the possible contribution by the dynamics of the ordered charge stripes at $(3, -0.33, 0)$ [23, 24]. Note that even though there was a persisting static charge stripe contribution in the elastic signal in Fig. 2(b) at this Q value, in the inelastic signal the dynamical contribution is dominated by the magnetic intensity from the fluctuating spin stripes. Nonetheless, we have also performed the T-dependent inelastic scans at $E = 2$ meV at the spin stripe satellite position $(1.33, 0, 0)$ in Fig. 3(c) where the contribution from the dynamics of the ordered charge stripes is absent. Similar monotonous decrease of the Q-integrated $\chi''(\omega)$ is observed as presented in Fig. 3(d) as expected

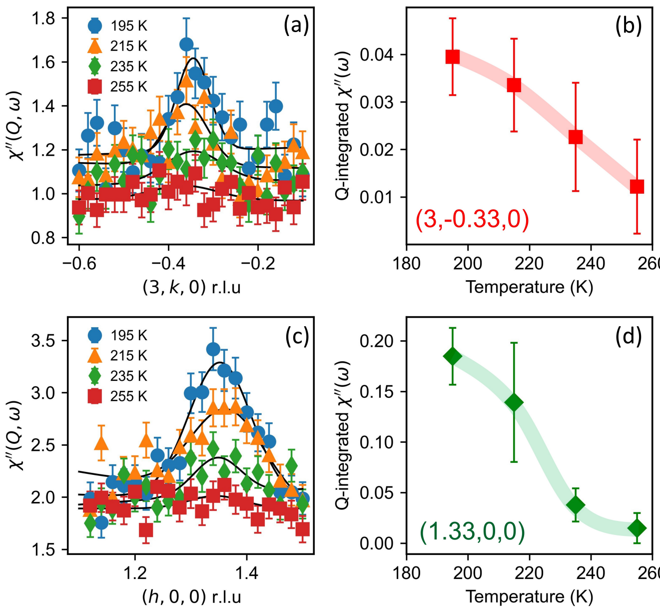

FIG. 3. (a) T-dependent inelastic scans through the spin and charge stripe overlapped satellite position at $(3, -0.33, 0)$ at $E = 3$ meV. (b) Corresponding plot of the Q-integrated dynamic susceptibility $\chi''(\omega)$ from the inelastic scans a function of temperature. (c) T-dependent inelastic scans through the spin stripe satellite position at $(1.33, 0, 0)$ at $E = 2$ meV. (d) Corresponding plot of the Q-integrated $\chi''(\omega)$ from the inelastic scans as a function of temperature. The inelastic scans are Bose corrected. Fainted lines are guide to eye.

following the magnetic form factor. This confirms unambiguously that the dominated magnetic character of the observed inelastic signal above T_{so} at $(3, -0.33, 0)$ is from the spin stripe fluctuations even when the satellite position is a spin and charge stripe overlapped position. The fluctuations of the spin stripes are strongly diminished close to the charge stripe melting temperature T_{co}. Since we have performed our inelastic measurements just above the spin stripe ordering temperature $T_{so} \approx 190$ K and below the charge stripe ordering temperature $T_{co} \approx 255$ K, the static charge stripe correlation should persist. Hence a dynamics related to the ordered charge stripes should be detectable but only possibly at much higher Q values *e.g.* as reported in $La_{1.75}Sr_{0.25}NiO_4$ at $(4.44, 3, 0)$ with $Q = 6.26$ Å^{-1} [24], and in $La_{1.66}Sr_{0.33}NiO_4$ at $(-1, 7.67, 0)$ with $Q = 9.03$ Å^{-1} [23]. However our previous INS studies on the $Pr_{1.5}Sr_{0.5}NiO_4$ show that the dynamics related to the ordered charge stripes at $(\pm 0.2, 3, 0)$ with $Q = 3.51$ Å^{-1} at 10 K is no longer detectable already beyond 3 meV in the inelastic map [29].

For our investigation of the spin stripe fluctuations above the spin stripe melting temperature T_{so} and to determine simultaneously their possible interaction with the concomitant charge stripe correlation in the same (Q, E)-range we have performed the inelastic scans at the spin and charge stripe overlapped satellite position

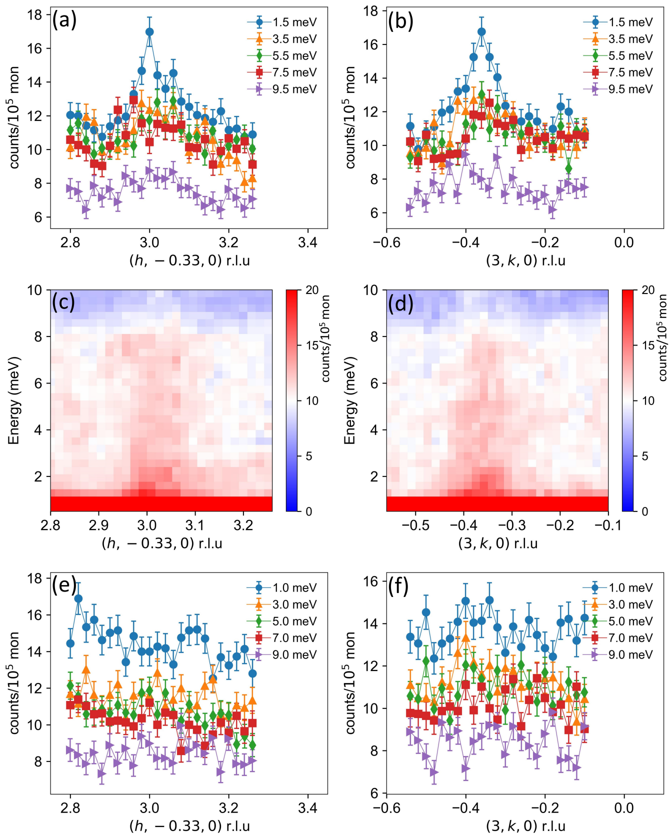

FIG. 4. (a,b) Spin stripe fluctuations measured along h and k directions at $(3, -0.33, 0)$ at 195 K just above T_{so}. (c,d) The respective color maps of the spin stripe fluctuations. (e,f) Spin stripe fluctuations measured along h and k directions at $(3, -0.33, 0)$ at 245 K close to T_{co}.

$(3, -0.33, 0)$. The choice of this satellite potions was also very helpful to avoid strong scattering intensities from the crystalline electric field (CEF) of Pr^{3+} ion at lower Q [30]. The constant-E scans at $(3, -0.33, 0)$ were performed in the energy interval of 0.5 meV upto 10 meV energy transfer at 195 K just above the T_{so} where no longer static spin stripe correlation persists. Fig. 4(a) presents selected set of constant-E scans. It is noticeable that with energy transfer the background intensities of the scans change. We relate this to the CEF level of the Pr^{3+} at ≈ 8 meV with a Gaussian distribution in energy which is reflected in the background intensities of the scans (see Fig. S2 in supplementary information [26]). Such CEF level is also observed in our previous INS studies on $Pr_{1.5}Sr_{0.5}NiO_4$ and $Pr_2NiO_{4+\delta}$ ($\delta = 0.24$) [29–32]. Similarly we have performed another set of constant-E scans in the perpendicular direction k in the same energy interval of 0.5 meV upto 10 meV energy transfer as presented in Fig. 4(b). All the scans were performed in the step size of 0.025 r.l.u. For a convenient visualization we have presented the inelastic intensities in the color maps in Fig. 4(c,d) respectively.

From the color maps it is apparent that the fluctuations can be detectable maximum upto 10 meV. Fig. 4(c,d) clearly present the non-dispersive character of the spin stripe fluctuations, as the scattering intensities remain broadly distributed around the incommensurate wave vector position. Here it is important to mention that the charge stripe fluctuations reported above the spin stripe melting temperature in the $La_{1.75}Sr_{0.25}NiO_4$ show rather a dispersive nature with a clear anisotropy indicating the presence of electron nematic order [24]. However, we were unable to observe any significant anisotropy of the spin stripe fluctuations along h and k directions *i.e.* in the parallel and perpendicular directions of the spin stripes in Fig. 4(c,d). It is notable that we have not seen any anomalous behaviour in the spin stripe fluctuations suggesting a significant interaction between the spin stripe fluctuations and the dynamical charge stripe. Nonetheless the peak position of the non-dispersive spin stripe fluctuations did not shift in Q, leaving the incommensurability of the stripes invariant which suggests that the spin and charge stripes can maintain an instantaneous correlation even when the static spin stripe order is absent above T_{so}. Such instantaneous correlation in between the spin and charge stripes has also been observed in time resolved x-ray diffraction studies [33, 34].

We have repeated some of the constant-E scans at the selected energies in between the 1 to 9 meV along the h and k directions at 245 K well below the T_{co} as presented in Fig. 4(e,f). In this temperature the static charge stripes are expected to be present but only with a very short range correlation. The constant-E scans show only a flat signal without any perceivable intensities at the incommensurate peak position corresponding to the spin stripe fluctuations. However one can identify immediately the changing background levels of the scans which is related to the CEF level and define a Gaussian with a peak at around 8 meV (see Fig. S2 in supplementary [26]). Nonetheless the high temperature scans in Fig. 4(e,f) show that the spin stripe fluctuations are strongly diminished as the static charge stripe correlation starts to vanish close to the T_{co} [6, 7]. This clearly indicates that static charge stripe order is essential for the dynamical spin stripe correlation to exist. On the other hand as the intensity of the spin stripe fluctuations vanishes already below the T_{co} it is apparent that the formation of the static charge order is not driven by the spin stripe fluctuations. This understanding is also consistent with the resonant x-ray photon correlation spectroscopy study on stripe formation in $La_{2-x}Sr_xNiO_{4+\delta}$ [35].

IV. CONCLUSION

In summary, we have investigated the spin stripe fluctuations in $Pr_{2-x}Sr_xNiO_{4+\delta}$ with $\epsilon = 0.33$ above the spin stripe melting temperature $T_{so} \approx 190$ K. The fluctuations are non-dispersive indicating a persisting instantaneous spin and charge stripe correlation above T_{so} and can be detected upto 10 meV. The spin stripe fluctuations are strongly diminished already below the charge stripe melting temperature $T_{co} \approx 255$ K, which clearly indicates that the formation of static charge order is not driven by spin stripe fluctuations, rather it suggests that the presence of static charge stripe order is a prerequisite for the spin stripe fluctuations to exist. The presence of spin stripe fluctuations has been suggested to promote the high temperature superconductivity in the antiferromagnetic high-T_c cuprates and therefore the knowledge about the microscopic route towards the spin stripe fluctuations remains crucial. Although 214-nickelates are not superconducting, however our results are important for elucidating the essential ingredients for spin stripe fluctuations. Such understanding may give key information about the competition between the antiferromagnetically ordered spin stripes and superconductivity. Therefore our findings are interesting to anticipate the role of spin stripe fluctuations in the mechanism of unconventional superconductivity as discussed in the high-T_c cuprates.

ACKNOWLEDGEMENTS

Authors would like to greatly acknowledge the support of Heinz Maier-Leibnitz Zentrum (MLZ), Technische Universität München in providing the neutron beam time at the thermal triple-axis spectrometer PUMA.

[1] J. M. Tranquada, B. J. Sternlieb, J. D. Axe, Y. Nakamura, and S. Uchida, Nature **375**, 561 (1995).

[2] N. B. Christensen, D. F. McMorrow, H. M. Rønnow, B. Lake, S. M. Hayden, G. Aeppli, T. G. Perring, M. Mangkorntong, M. Nohara, and H. Takagi, Phys. Rev. Lett. **93**, 147002 (2004).

[3] B. Vignolle, S. M. Hayden, D. F. McMorrow, H. M. Rønnow, B. Lake, C. D. Frost, and T. G. Perring, Nature Physics **3**, 163 (2007).

[4] M. Matsuda, M. Fujita, S. Wakimoto, J. A. Fernandez-Baca, J. M. Tranquada, and K. Yamada, Phys. Rev. Lett. **101**, 197001 (2008).

[5] J. M. Tranquada, D. J. Buttrey, V. Sachan, and J. E. Lorenzo, Phys. Rev. Lett. **73**, 1003 (1994).

[6] J. M. Tranquada, P. Wochner, and D. J. Buttrey, Phys. Rev. Lett. **79**, 2133 (1997).

[7] P. Bourges, Y. Sidis, M. Braden, K. Nakajima, and J. M. Tranquada, Phys. Rev. Lett. **90**, 147202 (2003).

[8] M. E. Ghazi, P. D. Spencer, S. B. Wilkins, P. D. Hatton, D. Mannix, D. Prabhakaran, A. T. Boothroyd, and S.-W. Cheong, Phys. Rev. B **70**, 144507 (2004).

[9] H. Woo, A. T. Boothroyd, K. Nakajima, T. G. Perring, C. D. Frost, P. G. Freeman, D. Prabhakaran, K. Yamada, and J. M. Tranquada, Phys. Rev. B **72**, 064437 (2005).

[10] P. G. Freeman, A. T. Boothroyd, D. Prabhakaran, C. D. Frost, M. Enderle, and A. Hiess, Phys. Rev. B **71**, 174412 (2005).

[11] H. Yoshizawa, T. Kakeshita, R. Kajimoto, T. Tanabe, T. Katsufuji, and Y. Tokura, Phys. Rev. B **61**, R854 (2000).

[12] R. Kajimoto, K. Ishizaka, H. Yoshizawa, and Y. Tokura, Phys. Rev. B **67**, 014511 (2003).

[13] S. A. Kivelson, E. Fradkin, and V. J. Emery, Nature **393**, 550 (1998).

[14] B. O. Wells, Y. S. Lee, M. A. Kastner, R. J. Christianson, R. J. Birgeneau, K. Yamada, Y. Endoh, and G. Shirane, Science **277**, 1067 (1997).

[15] V. Hinkov, D. Haug, B. Fauqué, P. Bourges, Y. Sidis, A. Ivanov, C. Bernhard, C. T. Lin, and B. Keimer, Science **319**, 597 (2008), https://www.science.org/doi/pdf/10.1126/science.1152309.

[16] T. Dahm, V. Hinkov, S. V. Borisenko, A. A. Kordyuk, V. B. Zabolotnyy, J. Fink, B. Büchner, D. J. Scalapino, W. Hanke, and B. Keimer, Nature Physics **5**, 217 (2009).

[17] K. Sun, M. J. Lawler, and E.-A. Kim, Phys. Rev. Lett. **104**, 106405 (2010).

[18] Y. Yamakawa and H. Kontani, Phys. Rev. Lett. **114**, 257001 (2015).

[19] F. Krüger and S. Scheidl, Phys. Rev. B **67**, 134512 (2003).

[20] E. W. Carlson, D. X. Yao, and D. K. Campbell, Phys. Rev. B **70**, 064505 (2004).

[21] D. X. Yao and E. W. Carlson, Phys. Rev. B **75**, 012414 (2007).

[22] A. M. M. Abeykoon, E. S. Božin, W.-G. Yin, G. Gu, J. P. Hill, J. M. Tranquada, and S. J. L. Billinge, Phys. Rev. Lett. **111**, 096404 (2013).

[23] S. Anissimova, D. Parshall, G. D. Gu, K. Marty, M. D. Lumsden, S. Chi, J. A. Fernandez-Baca, D. L. Abernathy, D. Lamago, J. M. Tranquada, and D. Reznik, Nature Communications **5**, 3467 (2014).

[24] R. Zhong, B. L. Winn, G. Gu, D. Reznik, and J. M. Tranquada, Phys. Rev. Lett. **118**, 177601 (2017).

[25] O. Sobolev and J. T. Park, Journal of large-scale research facilities **1**, A13 (2015).

[26] See the Supplementary at [URL will be inserted by publisher] for more details regarding elastic scans of spin and charge stripe satellites at different Brilloin zones and determination CEF level in the background of the inelastic scans. (2022).

[27] J. M. Tranquada, G. D. Gu, M. Hücker, Q. Jie, H.-J. Kang, R. Klingeler, Q. Li, N. Tristan, J. S. Wen, G. Y. Xu, Z. J. Xu, J. Zhou, and M. v. Zimmermann, Phys. Rev. B **78**, 174529 (2008).

[28] P. G. Freeman, A. T. Boothroyd, D. Prabhakaran, D. González, and M. Enderle, Phys. Rev. B **66**, 212405 (2002).

[29] A. Maity, R. Dutta, and W. Paulus, Phys. Rev. Lett. **124**, 147202 (2020).

[30] R. Dutta, A. Maity, A. Marsicano, J. R. Stewart, M. Opel, and W. Paulus, Phys. Rev. B **105**, 195147 (2022).

[31] R. Dutta, A. Maity, A. Marsicano, J. R. Stewart, M. Opel, and W. Paulus, Phys. Rev. B **102**, 165130 (2020).

[32] A. Maity, R. Dutta, A. Marsicano, A. Piovano, J. R. Stewart, and W. Paulus, Phys. Rev. B **103**, L100401 (2021).

[33] Y. D. Chuang, W. S. Lee, Y. F. Kung, A. P. Sorini, B. Moritz, R. G. Moore, L. Patthey, M. Trigo, D. H. Lu, P. S. Kirchmann, M. Yi, O. Krupin, M. Langner, Y. Zhu, S. Y. Zhou, D. A. Reis, N. Huse, J. S. Robinson, R. A. Kaindl, R. W. Schoenlein, S. L. Johnson, M. Först, D. Doering, P. Denes, W. F. Schlotter, J. J. Turner, T. Sasagawa, Z. Hussain, Z. X. Shen, and T. P. Devereaux, Phys. Rev. Lett. **110**, 127404 (2013).

[34] Y. F. Kung, W.-S. Lee, C.-C. Chen, A. F. Kemper, A. P. Sorini, B. Moritz, and T. P. Devereaux, Phys. Rev. B **88**, 125114 (2013).

[35] Y. Shen, G. Fabbris, H. Miao, Y. Cao, D. Meyers, D. G. Mazzone, T. A. Assefa, X. M. Chen, K. Kisslinger, D. Prabhakaran, A. T. Boothroyd, J. M. Tranquada, W. Hu, A. M. Barbour, S. B. Wilkins, C. Mazzoli, I. K. Robinson, and M. P. M. Dean, Phys. Rev. Lett. **126**, 177601 (2021).